Adenosine Mimetics as Inhibitors of NAD$^+$-Dependent Histone Deacetylases, from Kinase to Sirtuin Inhibition

Johannes Trapp,[†] Anne Jochum,[‡] Rene Meier,[§] Laura Saunders,[||] Brett Marshall,[||] Conrad Kunick,[⊥] Eric Verdin,[||] Peter Goekjian,[‡] Wolfgang Sippl,[§] and Manfred Jung[†,*]

Institute of Pharmaceutical Sciences, Albert-Ludwigs-Universität Freiburg, Albertstrasse 25, 79104 Freiburg, Germany, LCO2-Glycochimie, UMR 5181 Méthodologie de Synthèse et Molécules Bioactives, Université Claude Bernard Lyon 1, 43 Bd du 11 Novembre 1918, 69622 Villeurbanne Cedex, France, Department of Pharmaceutical Chemistry, Martin-Luther Universität Halle-Wittenberg, Wolfgang-Langenbeckstrasse 4, 06120 Halle/Saale, Germany, Gladstone Institute of Virology and Immunology, University of California, 1650 Owens Street, San Francisco, California 94158, and Institut für Pharmazeutische Chemie, Technische Universität Braunschweig, Beethovenstrasse 55, 38106 Braunschweig, Germany

Received February 3, 2006

NAD$^+$-dependent histone deacetylases, sirtuins, cleave acetyl groups from lysines of histones and other proteins to regulate their activity. Identification of potent selective inhibitors would help to elucidate sirtuin biology and could lead to useful therapeutic agents. NAD$^+$ has an adenosine moiety that is also present in the kinase cofactor ATP. Kinase inhibitors based upon adenosine mimesis may thus also target NAD$^+$-dependent enzymes. We present a systematic approach using adenosine mimics from one cofactor class (kinase inhibitors) as a viable method to generate new lead structures in another cofactor class (sirtuin inhibitors). Our findings have broad implications for medicinal chemistry and specifically for sirtuin inhibitor design. Our results also raise a question as to whether selectivity profiling for kinase inhibitors should be limited to ATP-dependent targets.

Introduction

Histone deacetylases (HDACs)[a] are enzymes that deacetylate histones and certain nonhistone proteins, thereby altering their conformational state or activity.[1] Three classes of histone deacetylases have been recognized in humans: class I and II are zinc-dependent amidohydrolases of which 11 subtypes have been discovered (HDAC1−11). Class III enzymes depend on NAD$^+$ for catalysis, and produce *O*-acetyl ADP ribose and nicotinamide (**1**) as a consequence of the acetyl transfer. Due to homology with the yeast histone deacetylase Sir2p, the NAD$^+$-dependent deacetylases are also termed sirtuins, and seven members (SIRT1−7) are known in humans.[2]

In the past few years a considerable amount of knowledge has accumulated on the biological activities of sirtuins.[2] They are linked to aging, and overexpression leads to an increased lifespan in yeast.[3] On the other hand, there are indications that sirtuins play a role in the pathogenesis of viral diseases[4] and cancer.[5−7]

While class I and II HDAC inhibitors are already investigated as new anticancer agents in clinical studies[8] much less is known about inhibitors of class III histone deacetylases. Only a few sirtuin inhibitors are available, and several of them do not inhibit human subtypes (Chart 1).[9,10] Nicotinamide (**1**) is the physiological sirtuin inhibitor. The first synthetic inhibitor discovered was sirtinol (**2**)[11] (Chart 1), and its hydrolysis product, 2-hydroxynaphthaldehyde, also shows some activity. At least in certain cases, precipitation of the sirtuin by sirtinol contributes to enzyme inhibition.[12] Structure−activity relationships of sirtinol analogues have been reported.[13] Another inhibitor, splitomicin (**3a**), was discovered as an inhibitor of yeast sirtuins[14] and is basically inactive on human subtypes. HR73 (**3b**) was derived from splitomicin by our group as the first selective (20-fold for SIRT1 over SIRT2) and potent inhibitor (IC_{50} < 5 μM) of human sirtuins[4] (See Chart 1). Two other inhibitors of SIRT2 were discovered using a virtual screening approach.[15] Sirtuin inhibitors with half-inhibitory concentrations as low as 98 nM have been reported recently.[16]

Chart 1. Known Inhibitors for Sirtuins

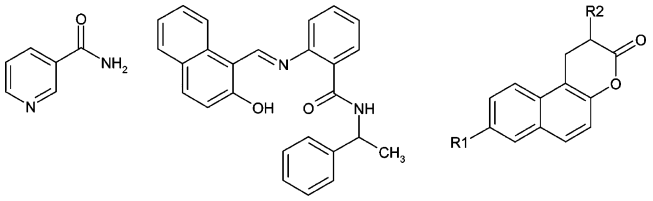

1 **2** **3a** R_1 = H; R_2 = H

3b R_1 = Br; R_2 = phenyl

Suramin and several related adenosine receptor antagonists inhibit sirtuins as well.[17] This prompted us to start a systematic investigation of sirtuin inhibition by drugs that target enzymes or receptors that bind adenosine-containing cofactors or ligands to identify lead structures for sirtuin inhibitors. Among these enzymes are kinases (using ATP) and dehydrogenases (using NAD$^+$). Certain kinase inhibitors, namely members of the paullone cyclin-dependent kinase (CDK) inhibitor series (e.g., kenpaullone), also inhibit NAD$^+$-dependent mitochondrial malate dehydrogenase (mMDH).[18] Thus, we tested a com-

* To whom correspondence should be addressed. E-mail: manfred.jung@pharmazie.uni-freiburg.de; Tel: +49-761-203-4896; Fax: +49-761-203-6321.
† Albert-Ludwigs-Universität Freiburg.
‡ Université Claude Bernard Lyon 1.
§ Martin-Luther Universität Halle-Wittenberg.
|| University of California.
⊥ Technische Universität Braunschweig.

[a] Abbreviations: HDAC: histone deacetylase; mMDH: mitochondrial malate dehydrogenase; CDK: cyclin-dependent kinase; BIM: bisindolylmaleimide; PKC: protein kinase C.

10.1021/jm060118b CCC: $33.50
Published on Web 11/10/2006

Chart 2. Structures of the Kinase Inhibitors Discovered in the Sirtuin Screening Showing SIRT2 Inhibitory Activity >60% at 12.5 μM

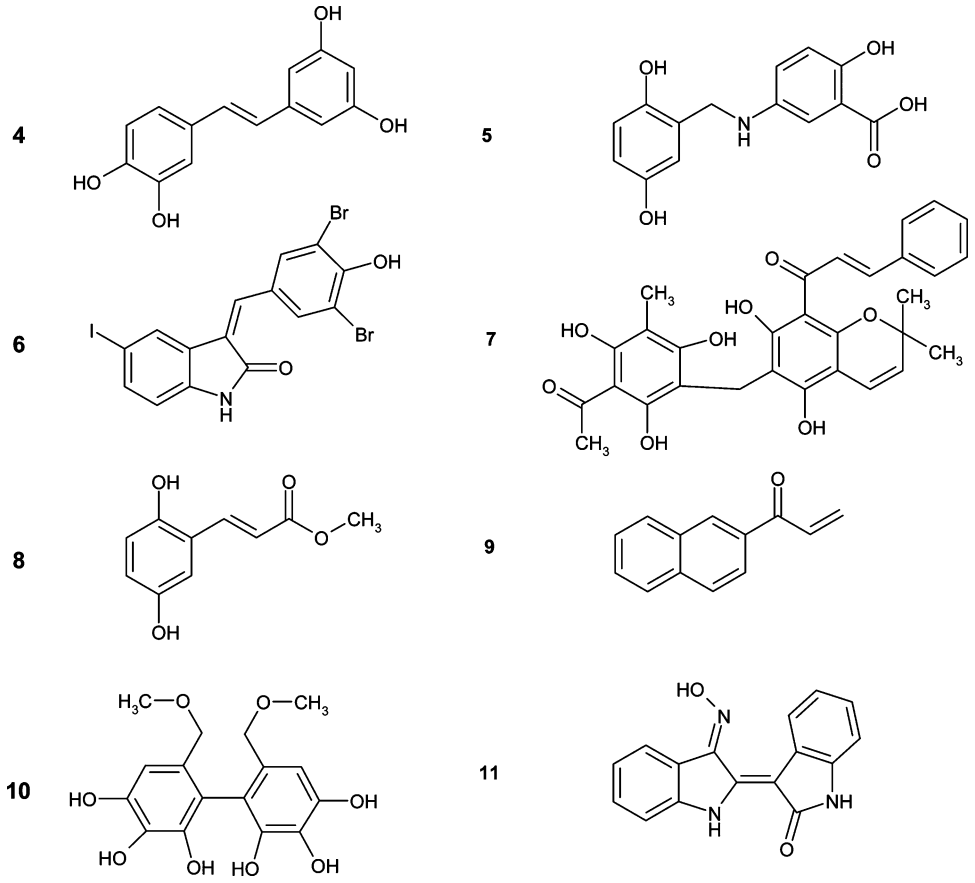

mercially available library of kinase and phosphatase inhibitors (84 compounds), containing inhibitors of various structural classes as well as CDK inhibitors (paullones), for their inhibitory potency toward SIRT2. We identified new lead structures for sirtuin inhibitors in several classes. Initial structure−activity relationships were obtained for the bisindolylmaleimide group of inhibitors (BIMs). The structural requirements for the binding of ATP-mimics to the NAD^+-binding site of sirtuins were investigated by means of molecular docking and analyzing favorable interaction fields using the program GRID.[19] Selected inhibitors from our screening were also investigated for selectivity toward SIRT1. Finally, hit validation was performed by investigating cellular hyperacetylation of α-tubulin, a SIRT2 substrate.

Results and Discussion

Enzyme Inhibition. To identify sirtuin inhibitors among adenosine mimics, we screened a commercially available kinase and phosphatase inhibitor library containing 84 compounds for in vitro enzyme inhibition. We used a homogeneous fluorescent assay,[20] developed in our group, that utilizes a fluorescent substrate for deacetylation[12] and a tryptic digestion step[21,22] to quantitate enzymatic conversion. We identified 10 compounds that had greater than 60% inhibition of SIRT2 at 12.5 μM, including the stilbene piceatannol (**4**), a benzoic acid derivative (**5**), the indolinone GW 5074 (**6**), rottlerin (**7**), an erbstatin analogue (**8**), the naphthylketone ZM 449829 (**9**), a biphenylpolyphenol (**10**), indirubin-3′-monooxime (**11**), and the two BIMs GF 109203X (**12h**) and Ro 31-8220 (**12j**) (see Charts 2 and 3). Nicotinamide (**1**) and sirtinol (**2**) were tested as reference compounds (Chart 1).

The active compounds can be grouped into potentially redox-active compounds **4**, **5**, **7**, **8**, and **10,** Michael acceptors **6**, **8**, **9**, and **11,** and indoles **6**, **11**, **12h**, and **12j** (see Charts 2 and 3). Because the first two groups are not ideal lead structures due to potential general bioreactivity, we focused on the indoles **12h** and **12j** for further investigations. The BIMs are a class of biologically active compounds originally identified in the 1980s as ATP-competitive protein kinase C (PKC) inhibitors.[23] Later work identified the macrocyclic BIMs, such as LY333531 (ruboxistaurin) as potent, isoform-selective inhibitors of PKC-beta, currently in phase III clinical trials for the treatment of diabetic complications.[24] We tested a set of BIMs **12a**−**k, 12m**, **13a**−**c**, and **14a**,**b** (see Charts 3−5) related to the lead structures **12h** and **12j** to obtain structure−activity relationships. We found that BIMs substituted on a single indole nitrogen (e.g., **12e**−**i**) were potent inhibitors of sirtuins and that these compounds were significantly more potent than either the macrocyclic BIMs (**12e** vs **13b**, **12g** vs **13a)** or the indolocarbazoles (staurosporine **14a**; Go6976 **14b**). In contrast, the structural features of **13** and **14** led to substantially increased activity against protein kinases.[25] Furthermore, BIMs bearing an alkyl group on the imide nitrogen, which are inactive against many protein kinases,[26−29] inhibit SIRT2 (**12b-d**): methyl (**12b**) and benzyl substitution (**12c**) decreased SIRT2 inhibition in comparison to the parent compound **12a**, but the IC_{50}-values of the most active *N*-alkyl compounds **12b** and **12c** (33 and 40 μM, respectively) were still in the range of the physiological inhibitor nicotinamide (**1**), determined to be 32.3 μM for SIRT2. Substituting the *N*-methyl BIM **12b** with simple alkyl or ω-hydroxyalkyl groups on both indole nitrogens was detrimental to activity (**12k, 12m**). However, substitution of the BIM **12a** with a cyclohexylidene-

Chart 3. Bis(indolyl)maleimides

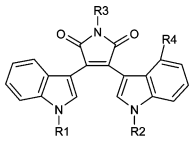

Compound	R1	R2	R3	R4
12a	H	H	H	H
12b	H	H		H
12c	H	H		H
12d				H
12e	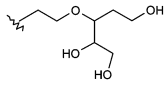	H	H	F
12f	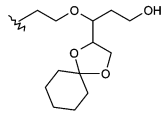	H	H	H
12g	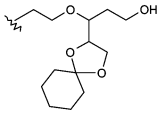	H	H	F
12h	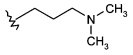	H	H	H
12i	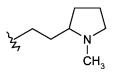	H	H	H
12j	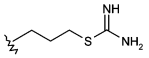		H	H
12k	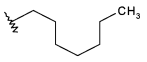	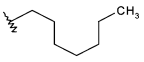		H
12l	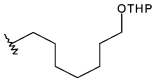	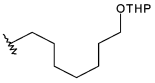		H
12m	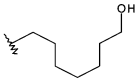	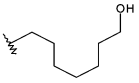		H

bearing alcohol chain as in **12f** and **12g** produced inhibitors with IC_{50} values of 2.8 and 2.5 μM, respectively, suggesting that potent inhibitors can be designed based on nonpolar motifs. The most active inhibitor was compound **12j**,[23] a disubstituted BIM bearing an isothiourea structure in the side chain at one indole nitrogen and a methyl substitution at the other, with an IC_{50} of 0.8 μM. This is one of the most potent sirtuin inhibitors described to date.

Because of their known affinity for the NAD^+-dependent mMDH and the presence of an indole moiety, we tested a set of three paullones for inhibition of SIRT2, including kenpaullone (**15a**), a potent inhibitor of CDKs[30] (see Chart 5). The prototype CDK inhibitor kenpaullone displayed a very low inhibition of Sirt2 at 100 μM, but benzylation of the lactam nitrogen (**15b**) or the introduction of a hydroxyamidine structure (**15c**) increased

Chart 4. Macrocyclic Bis(indolyl)maleimides

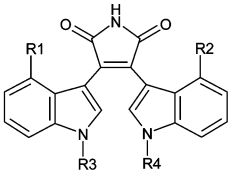

Compound	R1	R2	R3	R4
13a	F	H	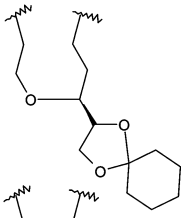	
13b	H	F	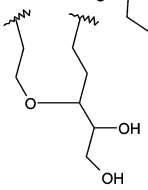	
13c	H	F	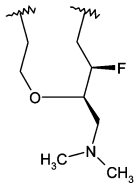	

Chart 5. Indolocarbazoles and Paullones

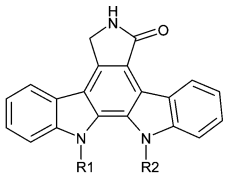

Compound	R1	R2
14a	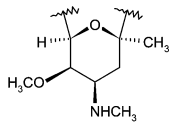	
14b	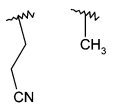	

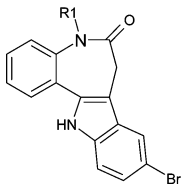

Compound	R1
15a	H
15b	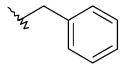
15c	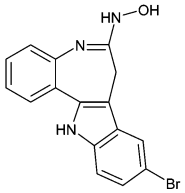

SIRT2 inhibition (see Table 1). Again, as in the BIM series, alkylation of the lactam nitrogen strongly reduces kinase inhibition,[30] but here increased activity against SIRT2.

Selected inhibitors **12a, 12b**, **12e**−**j, 13a-c**, and **15b** were also tested for SIRT1 inhibition (see Table 1). All the BIMs showed a marked selectivity toward SIRT2, while the paullone **15b** did not.

Competition analysis revealed that the best inhibitor **12j** is competitive with respect to NAD^+ (see Supporting Information). Competition with the fluorescent substrate can only be analyzed in a rather narrow concentration range due to substrate solubility problems, but the concentration window that we investigated shows no competition with the acetyl lysine derivative (data

Table 1. Sirtuin Inhibition

	% inhibition at concentration; IC_{50} greater than concentration or IC_{50} + SE [μM][a]	
no.	SIRT1	SIRT2 [μM]
1	10.6% @ 50 μM	32.3 ± 6.6
2	NT[b]	53.0 ± 15.8
12a	52.7 % @ 50 μM	4.7 ± 1.1
12b	>50	33.0 ± 5.2
12c	NT	40.0 ± 3.0
12d	NT	78.3 ± 18.2
12e	29.9% @ 50 μM	9.5 ± 1.5
12f	77.5% @ 50 μM	2.8 ± 1.2
12g	71.9% @ 50 μM	2.5 ± 0.6
12h	> 50	7.3 ± 2.4
12i	58.2% @ 50 μM	8.3 ± 0.5
12j	3.5 ± 0,4	0.8 ± 0.2
12k	NT	>100
12m	NT	>100
13a	55.7% @ 50 μM	20.8 ± 10.1
13b	NI[c] @ 50 μM	>50
13c	NI @ 50 μM	>50
14a	NT	NI @ 50 μM
14b	NT	>100
15a	NT	>100
15b	49.4% @ 50 μM	42.8 ± 17.9
15c	NT	43.1% @ 50 μM

[a] Values are means ± SE of duplicate experiments. [b] Not tested. [c] No inhibition.

Table 2. Inhibition of SIRT1 and -2 in Different Deacetylase Assays

	fluorimetric assay, IC50 [μM]		scintillation assay, IC50 [μM]	
compound	SIRT1	SIRT2	SIRT1	SIRT2
12b	>50	33.0	15.7	24.1
12h	>50	7.3	23.0	11.7
12j	3.5	0.8	5.1	1.1
15b	~50	42.8	8.0	10.0

Scheme 1. Synthesis of Bisalkylated BIMs

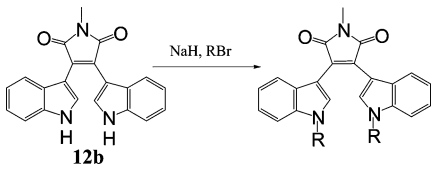

not shown). Thus, competition with the protein substrate cannot be ruled out completely, but its apparent lack agrees with the docking results (see below).

Because fluorescence-based deacetylase assays led to some false positives during a screen for sirtuin activators,[17,31,32] we tested selected inhibitors with another biochemical assay relying on scintillation counting after release of [^{3}H] acetic acid from the histone H4 N-terminal peptide (amino acids 1−25). This radioactive assay confirmed that BIMs and paullone **15b** are potent inhibitors of human sirtuins (Table 2). The results of the fluorescent and the radioactive assays are comparable. The scintillation assay identified the paullone **15b** as being more active on SIRT1 and -2 than in the fluorescent assay (8−10 μM vs 42.8 μM, respectively). Also **12h** was found to be more active in the radioactive assay. **12b** and **12h** did not show selectivity in the radioactive assay. The nature of the substrate (peptide vs small molecule) may influence the results. But, as the natural substrate is a histone in the context of a nucleosome or a nonhistone protein and not an isolated peptide, it remains to be determined which assay has the better predictive power

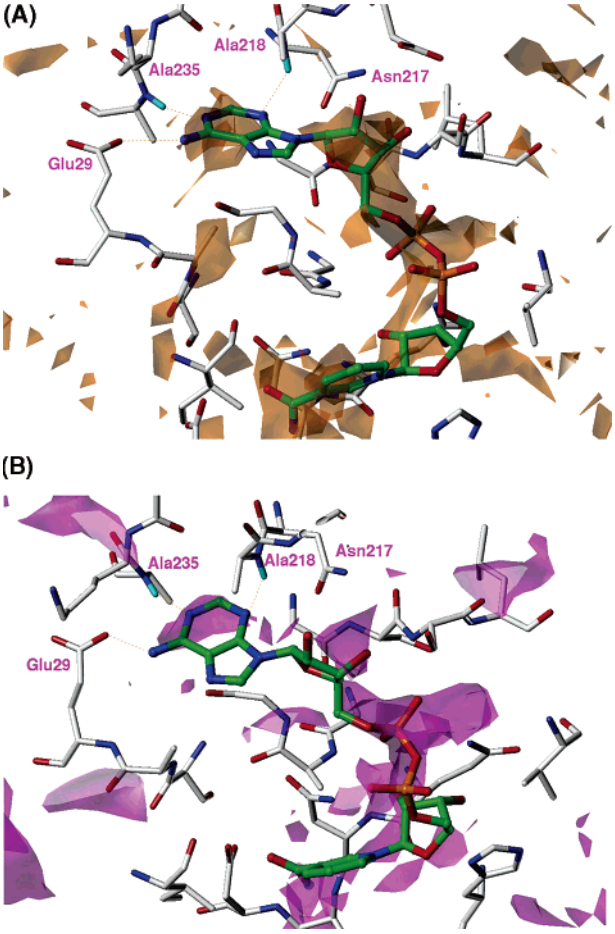

Figure 1. Sir2-Af2−NAD$^+$ complex. Interaction of NAD$^+$ (carbon atoms in green) with corresponding amino acid residues at the binding pocket. (a) The GRID interaction field obtained with the aromatic probe (contour level −2.5 kcal/mol, colored orange) is in perfect agreement with the aromatic adenine ring system. Hydrogens bonds between adenosine and SIRT2 are shown in orange. (b) The GRID field obtained with the carbonyl probe (contour level −4.5 kcal/mol, colored magenta) indicates the favorable hydrogen bond acceptor regions within the binding pocket.

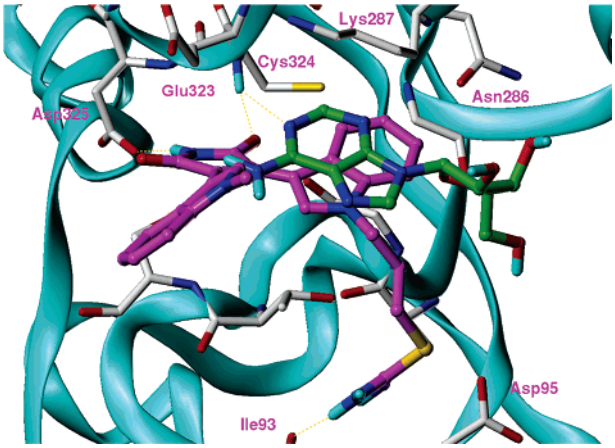

Figure 2. SIRT2−Ligand Complexes. Interaction of the adenosine part of NAD$^+$ (carbon atoms in green) and BIM **12j** (magenta) with the corresponding amino acid residues at the human SIRT2 binding pocket. Hydrogen bonds are shown in orange.

for cellular effects. **12j** is a potent inhibitor of SIRT2 in both assays with a four- to fivefold selectivity over SIRT1.

The conformational flexibility of the BIM moiety has allowed exquisite selectivity in terms of kinase inhibition, by constraining

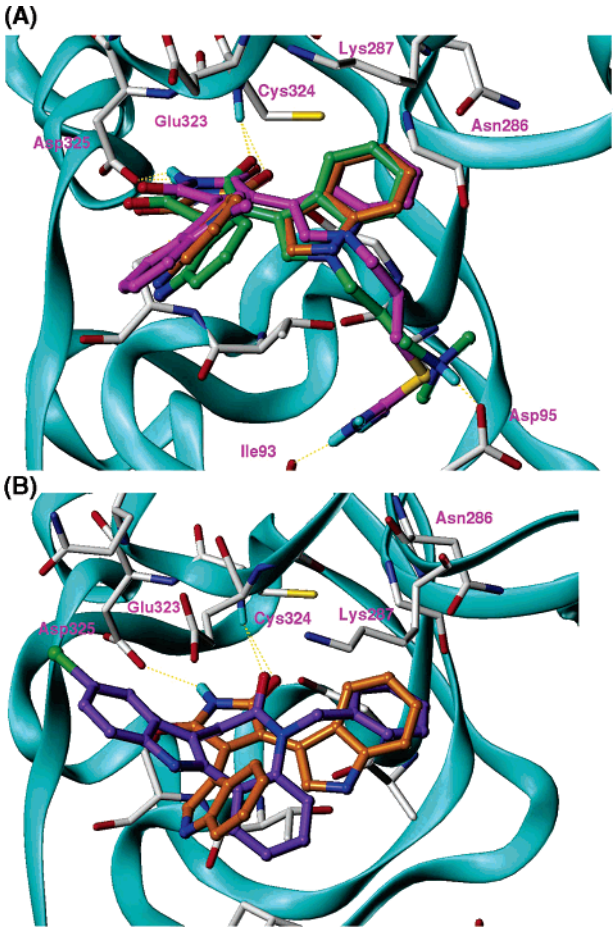

Figure 3. Docking results for BIMs. (a) Superimposition of docked inhibitors **12a** (orange), **12h** (green-blue) and **12j** (magenta). (b) Superimposition of docked inhibitors **12a** (orange) and paullone **15b** (purple). Hydrogen bonds are shown in orange.

the conformation. Our results demonstrate a similar potential for sirtuin inhibition. The BIMs are important lead compounds for the design of new, possibly subtype selective, sirtuin inhibitors.

Chemistry. The BIMs **12d** and **12k**,**l** were prepared by bisalkylation of the parent compound **12b** with alkyl bromides after deprotonation with NaH, followed by deprotection of the

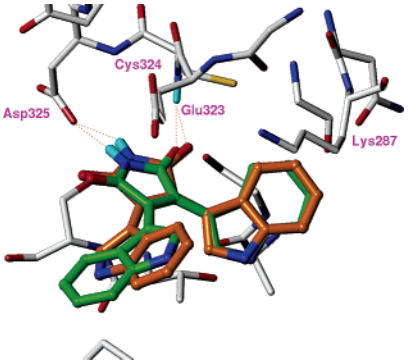

Figure 4. Docking results for BIM 12a. Comparison of the two favorable docking solutions obtained for inhibitor **12a**.

THP group in the case of **12m** (Scheme 1). The monosubstituted imides **12e**−**g** were prepared by adapting the method of Faul et al.[33] (Scheme 2). Alkylation of indole acetamide with the tosylate **16**,[34] followed by condensation of **17** with methyl 4-fluoroindole-3-glyoxylate and acidic workup, led to a mixture of the triol **12e** and the cyclohexylidene **12g**. The nonfluorinated compound **12f** was prepared by an analogous route using methyl indole-3-glyoxylate.[35]

Examination of the Putative Inhibitor Binding Site. All Sir2 structures contain a conserved catalytic domain of 270 amino acids with variable N- and C-termini. Consistent with the high sequence similarity in the catalytic domain, the available structural data on the Sir2 proteins also show conservation in the tertiary structure.[36,37] The structure of the catalytic domain consists of a large classical Rossmann-fold and a small zinc-binding domain. The acetylated peptide binds in the cleft between the two domains and forms an enzyme−substrate β-sheet with two flanking strands from the enzyme. The acetyl-lysine residue inserts into a conserved hydrophobic pocket, and NAD^+ binds nearby.[37] The interaction of NAD^+ at the binding pocket can be examined in several sirtuin X-ray structures in which the cofactor has been cocrystallized.[37,38] Structural comparison of available NAD^+−sirtuin complexes from the Protein Data Bank revealed a highly conserved and rigid NAD^+ binding site.[39]

First, by using the program GRID[19] the NAD^+ putative binding site was examined to determine possible favorable interactions. Since the NAD^+ molecule in human SIRT2 was

Scheme 2. Synthesis of Monoalkylated BIMs

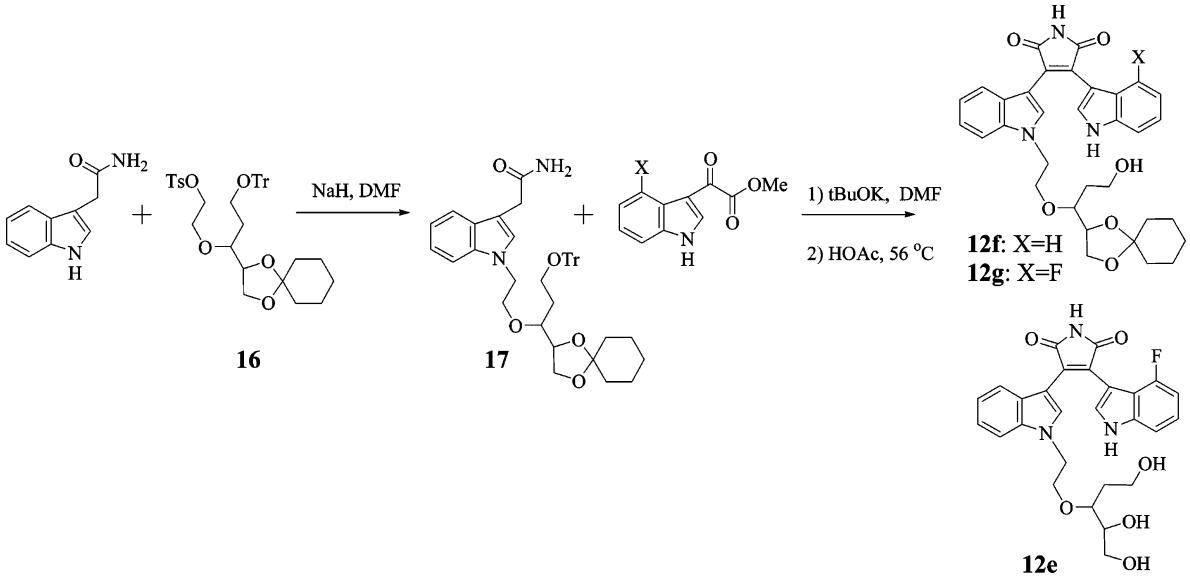

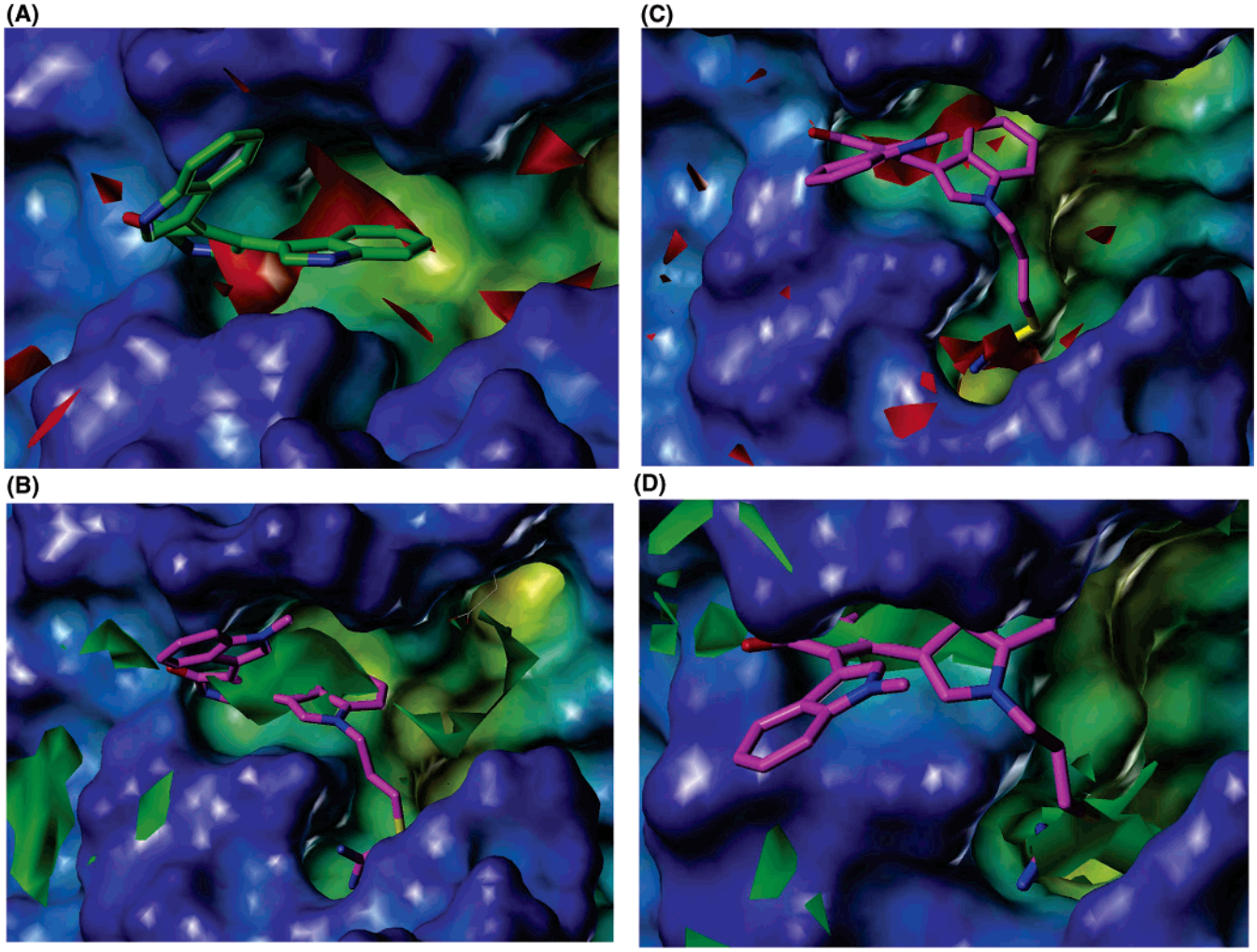

Figure 5. Favorable interaction fields (GRID) obtained with: (a) carbonyl probe (colored red at −4.5 kcal/mol), (b) aromatic probe (colored green at −3.0 kcal/mol), (c) amine probe (colored red at −8.0 kcal/mol), and (d) amidine probe (colored green at −10.0 kcal/mol). The docked inhibitors **12a** (colored green) and **12j** (colored magenta) are shown for comparison. The molecular surface of the binding pocket is calculated using the MOLCAD program colored according the cavity depth (blue = exposed, orange = buried).

not resolved, we analyzed the archaeal homologue Sir2-Af2.[37] The calculated GRID contour maps were superimposed on the crystal structure of Sir2-Af2 and compared with the positions of the cocrystallized NAD^+ molecule and the amino acids of the active site (Figure 1A and 1B). On the basis of GRID probes, the carbonyl group had an interaction energy of −5 kcal/mol near the backbone NH of Cys324 and Asp325. The amide NH probe yielded an interaction energy of −6 kcal/mol near the carboxyl groups of Asp325 and Glu323 (data not shown). The aromatic probe yielded a favorable interaction field between the aliphatic portions of Thr89, Lys287, and Glu323 in perfect agreement with the position of the aromatic adenine ring of NAD^+ as taken from the Sir2-Af2 X-ray structure (Figure 1A and 1B).[37] Because the NAD^+ binding site is highly conserved, similar GRID results were obtained for the human SIRT2 structure (data not shown).

Second, we tested whether the docking program GOLD[40] can reproduce the experimentally observed interaction of NAD^+ at Sir2-Af2. The NAD^+ molecule and the less flexible adenosine moiety were docked in the putative binding pocket near Cys324. The observed low heavy atom rmsd value between top-ranked docking solution and X-ray structure (0.75 Å for the adenosine fragment and 1.06 Å for the whole NAD^+ molecule) showed that GOLD can correctly predict the bioactive conformation of the adenosine moiety as well as for the complete NAD^+ (see Supporting Information). Similar results were obtained when the adenosine fragment was docked in the corresponding pocket of human SIRT2 (see Supporting Information). In the human sirtuin, the adenine ring of adenosine is surrounded by several residues (Gly86, Asn286, Lys287, Glu288, Glu323, Cys324, and Asp325, see Figure 1) similar to those observed in the X-ray structure of Sir2-Af2.[37]

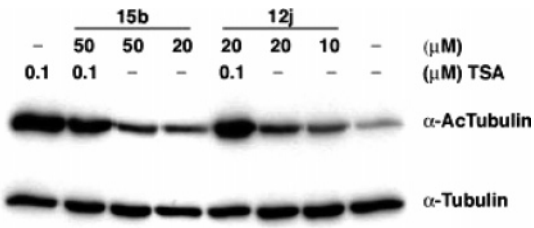

Figure 6. In vivo SIRT2 inhibition. A549 cells were treated with the indicated amounts of **12j**, **15b**, and TSA for 6 h and analyzed by western blotting with antibodies against acetylated α-tubulin and α-tubulin.

In a subsequent step, the inhibitors were docked into this well-defined binding pocket. The docking of the most potent inhibitor **12j** revealed a second putative binding site for the polar isothiourea group near Ile93 and Asp95 (Figure 2). The docking solutions of four other potent inhibitors are shown within the binding pocket in Figures 3A and 3B. As a relatively rigid compound, **12a** led to two reasonable docked conformations

which are in agreement with the GRID maps. The two docking solutions differ only in the orientation of one of the indole rings. Figure 4 shows **12a** bound in a folded and in a *C*2-symmetrical conformation. This observation has also been made for BIMs bound to kinases where different orientations of the indole rings can be observed.[41]

The planar ring systems of the docked inhibitors fit perfectly in the adenine-binding pocket and form hydrogen bonds with Cys324 and Asp325. The maleimide ring of the potent BIMs lies in a central position, in close proximity to Cys324. Due to the rigidity of staurosporine (**14a**), it was not possible to obtain a favorable docking solution within the adenine-binding pocket. Thus, a certain flexibility within the BIMs is needed so that the two indole rings can adopt the appropriate conformation. This observation is in agreement with the observed inactivity of compounds **14a** and **14b** against SIRT2.

The docking results showed that the active inhibitors can interact in similar ways with the adenine-binding pocket. However, on the basis of the docking results (i.e., Goldscore), no discrimination could be derived between more and less active inhibitors. This is often observed when dealing with docking scores.[42] Therefore, we focused on a qualitative analysis of key interactions necessary for high inhibitory activity.

A common feature of all docked inhibitors is the strong interaction of the aromatic ring moiety with the hydrophobic portions of residues Thr89, Lys287, Glu323, and Cys324. This type of interaction can also be observed for the adenine base of NAD^+. Figure 2 shows the superimposition of **12j** and the docked adenosine fragment. The indole ring of **12j** occupies the same region in space as the adenine ring of NAD^+. In addition, all docked active inhibitors show a strong hydrogen bond of the carbonyl group and the backbone NH of Cys324. The carbonyl groups are located in the same area as the favorable GRID interaction field of the carbonyl probe (Figure 5A), suggesting the importance of an interaction between the inhibitor's hydrogen bond acceptor group and the backbone NHs of Cys324.

The most potent BIMs bear an additional polar or basic side chain attached to one of the indole rings. This polar or basic group interacts with a second sub-pocket nearby Ile93 and Thr89. Favorable interactions within this subpocket were detected using the GRID amidine and amine probe (Figure 5A−D). The hydroxyl probe led to similar results as the amine probe (data not shown). The potent BIM derivatives interact with this second polar binding site by making electrostatic interactions with Asp95 (**12h**, **12i**) or by making hydrogen bonds to the backbone NH of Ile93 (**12j,** Figure 3). Due to the high flexibility of the two side chains of the inactive BIMs, **12k** and **12m**, no suitable docking results were obtained for these molecules.

Validation of Sirtuin Inhibition in Cell Culture. To evaluate the *in vivo* inhibition of SIRT2, compounds **12j** and **15b** were tested for their abilities to induce hyperacetylation of the SIRT2 target tubulin.[43] A549 human lung adenocarcinoma cells were treated with compounds **12j** and **15b** for 6 h. Western blot analysis using an antibody to the acetylated form of tubulin showed that compound **12j** and to a lesser extent **15b** induced hyperacetylation of tubulin (Figure 6). Tubulin was also hyperacetylated by 0.1 μM TSA, which inhibits class I and II HDACs, including the tubulin deacetylase HDAC6. Certain combinations of compound **12j** and **15b** with TSA did not induce greater levels of tubulin acetylation (Figure 6). More detailed studies would be necessary to prove or rule out additive or synergistic effects. Thus, compounds **12j** and **15b** inhibit SIRT2 *in vivo* and induce hyperacetylation of tubulin.

Conclusion

Random screening and target-fishing approaches had previously identified adenosine mimics, such as suramin, and kinase inhibitors, namely the paullones, as compounds that also target NAD^+-dependent enzymes. We developed a systematic approach to establish structure−activity relationships between selective inhibitors and different classes of enzymes that use adenosine-containing cofactors. We show that an overlap between ATP and NAD^+ mimesis by adenosine mimetics is more general than previously suspected. As several of the micromolar sirtuin inhibitors are more potent as kinase inhibitors, selectivity is most likely not an issue in those instances. Nevertheless, the first kinase inhibitors have already obtained approval as drugs, and as many more are in clinical trials, the investigation of selectivity should not be limited too readily to kinases. This is especially true for a potential inhibition of sirtuins due to their general involvement in aging.[44] Additionally, the IC_{50} values obtained for kinase inhibition are dependent on the ATP concentration used in the *in vitro* assays. Often these ATP concentrations are considerably lower than in the cell, and thus, such assays tend to overestimate kinase inhibitory potency.[29]

Our results have implications for sirtuin inhibitor design. We identified new lead structures in the low- or even submicromolar range. **12j** is one of the most potent sirtuin inhibitors reported to date. This supports the use of our nonradioactive screening assay as a tool for sirtuin inhibitor discovery. Among a series of related PKC inhibitors, only **12j** led to the induction of apoptosis at 10 μM,[45] and in this concentration range we observe cellular tubulin hyperacetylation. Although it is tempting to tie these proapoptotic properties to sirtuin inhibition, further studies are needed to substantiate these assumptions.

Additionally, with N-alkylation and in particular N-benzylation, we identified a promising structural descriptor for achieving sirtuin over kinase inhibition. Cell-permeable inhibitors, such as **12b** (bisindolylmaleimide V) and **12c**, that are inactive as inhibitors for most kinases,[29] may be useful for cellular studies aimed at determining the biological roles of sirtuins. These results provide the outline of a synthetic program aimed at combining features of sirtuin inhibition potency and selectivity for improved sirtuin inhibitor design. The modeled protein−inhibitor complexes will be a valuable tool toward this end.

Experimental Section

Materials. All chemicals were purchased from Sigma, Aldrich, or Fluka and used without further purification. The kinase and phosphatase inhibitor library was purchased from BIOMOL International.

Inhibitors. Paullones were synthesized as described (**15a**;[46] **15b**,**c**[30]). BIM **12c**[47] and macrocycles **13a**, **13b**, **13c** were synthesized as described.[34] **12a**,**b**, **12h**−**j**, and **14a**,**b** were purchased from Calbiochem.

General Procedure for the Synthesis of Bisindolylmaleimides 12d, **12k**, **12l.** To a solution of the bisindolylmaleimide (1 equiv) in DMF (400 μL/0.14 mmol) were added NaH (2.2 eq, 60% dispersion in mineral oil) and the alkyl halide (2 equiv). The mixture was stirred at room temperature for 2 h. The mixture was quenched with saturated aqueous NH_4Cl and extracted with CH_2Cl_2. The organic layer was washed with brine, dried over Na_2SO_4, filtered, and concentrated to dryness. Purification (SiO_2: 0−50% gradient of EtOAc in CH_2Cl_2) afforded the compound as a red solid (For NMR and purity data of all compounds, see Supporting Information).

12d: Yield 69%; MS (CI, isobutane) *m*/*z* 522 $^+$; HRMS (CI, isobutane) calcd for $C_{35}H_{28}N_3O_2$ 522.2182, found *m*/*z* 522.2183.

12k: Yield 30%; MS (CI, isobutane) *m/z* 538 $[MH]^+$; HRMS (CI, isobutane) calcd for $C_{35}H_{44}N_3O_2$ 538.3433, found *m/z* 538.3434.

12l: Yield 27%; MS (FAB, NBA) *m/z* 709 $[M]^+$; HRMS (CI, isobutane) calcd for $C_{43}H_{55}N_3O_6$ 709.4091, found *m/z* 709.4094.

Bisindolylmaleimide 12m. *p*-Toluenesulfonic acid (1 mg) was added to a solution of **12l** (27 mg, 0.04 mmol) in MeOH (1 mL). The mixture was stirred at room temperature for 2 h. The mixture was quenched with saturated aqueous NH_4Cl and extracted with EtOAC. The organic layer was washed with brine, dried over Na_2SO_4, filtered, and concentrated to dryness. Purification (SiO_2: 0−50% gradient of EtOAc in CH_2Cl_2) afforded **12m** (6 mg, 28%) as a red solid. MS (FAB, glycerol) *m/z* 541 $[M]^+$, 542 $[M + H]^+$; HRMS (FAB, glycerol) calcd for $C_{33}H_{39}N_3O_4$ 541.2941, found *m/z* 541.2942.

Indole Acetamide Derivative 17. To a solution of NaH (39 mg, 1.6 mmol, 60% dispersion in mineral oil) in DMF (300 μL) at 0 °C was added indole-3-acetamide (224 mg, 1.3 mmol), and the mixture was allowed to warm to room temperature and stir for 30 min. Tosylate **16**[34] (500 mg, 0.76 mmol) in DMF (300 μL) was added, and the reaction mixture was stirred at 70 °C for 18 h. The reaction was cooled to room temperature, quenched with saturated aqueous NH_4Cl, and diluted with EtOAc. The organic layer was washed with brine, dried over Na_2SO_4, filtered, and concentrated to dryness. Purification (SiO_2: EtOAc) led to the isolation of the indole acetamide derivative **17** (387 mg, 77%) as a yellow oil. MS (LSIMS, NBA) *m/z* 658 $[M]^+$, 681 $[M + Na]^+$; HRMS (LSIMS, NBA) calcd for $C_{42}H_{46}N_2O_5$ 658.3407, found *m/z* 658.3406.

Bisindolylmaleimides 12e and 12g. To a solution of **17** (400 mg, 0.61 mmol) and methyl 4-fluoroindole-3-glyoxylate (376 mg, 1.70 mmol)[33] in a mixture of THF:DMF (2:1, 5.7 mL) was added potassium *tert*-butoxide (3.60 mL, 1 M in THF, 3.6 mmol), and the reaction mixture was stirred at 70 °C for 5 h. The mixture was quenched with saturated aqueous NH_4Cl, and diluted with EtOAc. The organic layer was washed with H_2O, dried over Na_2SO_4, filtered, and concentrated to dryness to afford the alcohol (500 mg).

The alcohol (161 mg, 0.19 mmol) was dissolved in acetic acid (3 mL), and the reaction mixture was stirred at 56 °C for 6 h. The mixture was quenched with H_2O and diluted with EtOAc. The organic layer was washed with brine and saturated aqueous $NaHCO_3$, dried over Na_2SO_4, filtered, and concentrated to dryness. Purification (SiO_2: 100% EtOAc) afforded the cyclohexylidene **12g** (45 mg, 39%) as a red oil and the diol **12e** (6 mg, 8%) as a red oil.

12g: MS (LSIMS, thioglycerol) *m/z* 587 $[M]^+$; HRMS (LSIMS, thioglycerol) calcd for $C_{33}H_{34}FN_3O_6$ 587.2431, found *m/z* 587.2434.

12e: MS (LSIMS, thioglycerol) *m/z* 507 $[M]^+$, 508 $[MH]^+$; HRMS (LSIMS, thioglycerol) calcd for $C_{27}H_{26}FN_3O_6$ 507.1806, found *m/z* 507.1805.

Bisindolylmaleimide 12f. The nonfluorinated bisindolylmaleimide **12f** was prepared by the same procedure. **12f** (Yield: 17%): MS (LSIMS, glycerol) *m/z* 569 $[M]^+$; HRMS (LSIMS, glycerol) calcd for $C_{33}H_{35}N_3O_6$ 569.2526, found *m/z* 569.2524.

Molecular Modeling. All calculations were performed on a Pentium IV 1.8 GHz based Linux cluster. The molecular structures of the inhibitors were generated using the MOE modeling package (Chemical Computing Group).[48] The structures were energy minimized using the MMFF94s force field and the conjugate gradient method, until the default derivative convergence criterion of 0.01 kcal/(mol Å) was met. The crystal structures of human SIRT2 (pdb code 1J8F)[36] and archaeal Sir2-Af2(pdb code 1YC2)[37] were taken from the Protein Data Bank. SIRT2 is a monomer in solution, and therefore only chain B was chosen from the trimeric SIRT2 structure of 1J8F. Monomer B was selected for SIRT2 and monomer C for Sir2-Af2, as they showed the best stereochemical quality examined with the program PROCHECK.[49] In addition to the uncomplexed form of human SIRT2, the archaeal Sir2-Af2 crystal structure was used for the current investigation to inspect the NAD^+−enzyme interaction. Since the X-ray structures might contain residual energetic tensions from the crystallization process, both structures were first energy minimized. After removal of the cocrystallized water molecules and addition of hydrogen atoms to the protein structure, a descent minimization using the MMF94s force field and the GB/SA continuum[50] solvent model for water was carried out. During the minimization, a tethering constant of 100 kcal/(mol Å) on the backbone atoms was applied, after a stepwise reduction of the tethering to 1 kcal/(mol Å).

Interaction possibilities were analyzed using the GRID program (Molecular Discovery Inc.). GRID is an approach to predict noncovalent interactions between a molecule of known three-dimensional structure (i.e., a sirtuin) and a small group as a probe (representing chemical features of a ligand).[19] The calculations were performed using version 22 of the GRID program and the crystal structures mentioned above. The calculations were performed on a cube (20 × 20 × 20 Å, spacing 1 Å), including the NAD^+ binding pocket, to search for binding sites complementary to the functional groups of the inhibitors. The following probes were used for calculation: carbonyl, aromatic, amidine, and amine probes. The calculated GRID contour maps were then viewed superimposed on the crystal structure of the sirtuins with the MOE program.

Docking of the cocrystallized NAD^+ and adenosine, as well as the tested inhibitors, was carried out using program GOLD 2.3.[40] All torsion angles in each compound were allowed to rotate freely. Goldscore was chosen as the fitness function. For each molecule, 30 docking runs were performed. The resulting solutions were clustered on the basis of the heavy atom rmsd values (0.75 Å). The top-ranked poses for each ligand were retained and viewed graphically within MOE. The docking solution that showed the best agreement with the calculated GRID maps was manually selected for each inhibitor.

Recombinant Proteins. Human SIRT2 (N-terminally tagged with 6 His) was prepared as described[51] with minor modifications. In brief, the plasmid pEV1440, containing the full-length human SIRT2 cDNA was transformed in *Escherichia coli* strain BL21 for expression. The culture was grown in LB medium to an optical density of 0.6 (A_{600}) at 37 °C, induced with 0.1 mM IPTG for 2 h, and pelleted. Lysis was performed with a French press. The soluble overexpressed recombinant protein was purified using Ni-NTA resin. The identity of the produced His-SIRT2 was verified by SDS electrophoresis. Deacetylase activity of the produced SIRT2 was dependent on NAD^+ and could be inhibited with sirtinol and nicotinamide. The human sirtuin hSIRT1 was purchased from Biomol (activity: 3.5 U/μL).

Fluorescent Deacetylase Assay. All compounds were evaluated for their abilities to inhibit recombinant sirtuins in a homogeneous fluorescent deacetylase assay.[20] Stock solutions of inhibitors were prepared in DMSO, and 3 μL or less of a suited DMSO inhibitor solution was added to the incubation mixture. The assay was carried out in 96-well plates: 60 μL reaction volume contained the fluorescent histone deacetylase substrate ZMAL (10.5 μM), NAD^+ (500 μM), and Sirt2 (3 μL) or Sirt1 (1.2 μL). After 4 h of incubation at 37 °C, the deacetylation reaction was stopped, and the metabolite ZML (deacetylated form of ZMAL) was developed using a tryptic digest to form a fluorophore. Fluorescence was measured in a plate reader (BMG Polarstar) with a coumarin filter (excitation 390 nm and emission 460 nm). The amount of remaining substrate in the positive control with inhibitor versus negative control without inhibitor was employed to calculate inhibition. All determinations were carried out at least in duplicate. IC_{50} data were analyzed using GraphPad Prism Software.

Radioactive Deacetylase Assay. The deacetylase assay with recombinant SIRT1 and 2 was performed as described. [^{3}H]-Acetylated H4 histone N-terminal peptide (residues 1−25) was used as peptide substrate.[51]

Analysis of Tubulin Acetylation. A549 human lung carcinoma cells were cultured in Dulbecco's modified Eagle's medium (DMEM; Mediatech, Herndon, VA) supplemented with 10% fetal bovine serum (Gemini Bio-products, Woodland, CA), 1% penicillin−streptomycin, and 2 mM l-glutamine (GIBCO Invitrogen Corporation). A549 cells (50K/well) were plated in 12-well dishes 1 day before treatment with 12j, 15b, and Trichostatin A (TSA; Wako Chemicals USA, Richmond, VA). After 6 h of treatment, cells were washed with PBS and lysed in 50 mM Tris-HCl, pH 7.5, 0.5 mM EDTA, 150 mM NaCl, 0.5% NP-40, 400 nM TSA,

10 mM nicotinamide, and 1x complete protease inhibitors (Roche, Penzberg, Germany). Protein concentration was determined with the D_C Protein Assay (Bio-Rad). Protein samples were separated by electrophoresis on 10% SDS-polyacrylamide gels and transferred to a nitrocellulose membrane (Bio-Rad). Membranes were blocked with 5% nonfat dry milk in TBS-Tween (10 mM Tris-HCl, pH 7.5, 150 mM NaCl, and 0.1% Tween-20) and probed with anti-acetylated α-tubulin (6-11B-1; Sigma) and anti-α-tubulin (B-5-1-2; Sigma) at 1:2000.

Acknowledgment. Funding by the European Commission (Contract No LSHB-CT-2004-503467, to P.G. and C.K.) and the Albert-Ludwigs-University of Freiburg (Wilhelm-Seiter-Stiftung and Eugen-Graetz-Preis, to M.J.) is gratefully acknowledged.

Supporting Information Available: Additional spectral data for compounds **12d**−**m** and **17** and information on compound purity, kinetic analysis, and docking studies. This material is available free of charge via the Internet at http://pubs.acs.org.

References

(1) Grozinger, C. M.; Schreiber, S. L. Deacetylase enzymes: Biological functions and the use of small-molecule inhibitors. *Chem. Biol.* **2002**, *9*, 3−16.
(2) North, B. J.; Verdin, E. Sirtuins: Sir2-related NAD-dependent protein deacetylases. *Genome Biol.* **2004**, *5*, 224.
(3) Imai, S.; Armstrong, C. M.; Kaeberlein, M.; Guarente, L. Transcriptional silencing and longevity protein Sir2 is an NAD- dependent histone deacetylase. *Nature* **2000**, *403*, 795−800.
(4) Pagans, S.; Pedal, A.; North, B. J.; Kaehlcke, K.; Marshall, B. L. et al. SIRT1 Regulates HIV Transcription via Tat Deacetylation. *PLoS Biol.* **2005**, *3*, e41.
(5) Vaziri, H.; Dessain, S. K.; Ng, Eaton, E.; Imai, S. I.; Frye, R. A. et al. hSIR2(SIRT1) functions as an NAD-dependent p53 deacetylase. *Cell* **2001**, *107*, 149−159.
(6) Bereshchenko, O. R.; Gu, W.; Dalla-Favera, R. Acetylation inactivates the transcriptional repressor BCL6. *Nat. Genet.* **2002**, *32*, 606−613.
(7) Ota, H.; Tokunaga, E.; Chang, K.; Hikasa, M.; Iijima, K. et al. Sirt1 inhibitor, Sirtinol, induces senescence-like growth arrest with attenuated Ras-MAPK signaling in human cancer cells. *Oncogene* **2005**.
(8) Johnstone, R. W. Histone-deacetylase inhibitors: novel drugs for the treatment of cancer. *Nat. Rev. Drug Discovery* **2002**, *1*, 287−299.
(9) Schäfer, S.; Jung, M. Chromatin modifications as targets for new anticancer drugs. *Arch. Pharm. Chem. Life Sci.* **2005**, *338*, 347−357.
(10) Biel, M.; Wascholowski, V.; Giannis, A. Epigenetics - An epicenter of gene regulation: Histones and histone-modifying enzymes. *Angew. Chem., Int. Ed.* **2005**, *44*, 3186−3216.
(11) Grozinger, C. M.; Chao, E. D.; Blackwell, H. E.; Moazed, D.; Schreiber, S. L. Identification of a class of small molecule inhibitors of the sirtuin family of NAD-dependent deacetylases by phenotypic screening. *J. Biol. Chem.* **2001**, *276*, 38837−38843.
(12) Heltweg, B.; Dequiedt, F.; Verdin, E.; Jung, M. A non isotopic substrate for assaying both human zinc and NAD^+-dependent histone deacetylases. *Anal. Biochem.* **2003**, *319*, 42−48.
(13) Mai, A.; Massa, S.; Lavu, S.; Pezzi, R.; Simeoni, S. et al. Design, synthesis and biological evaluation of sirtinol analogues as class III histone/protein deacetylase (sirtuin) inhibitors. *J. Med. Chem.* **2005**, *48*, 7789−7795.
(14) Bedalov, A.; Gatbonton, T.; Irvine, W. P.; Gottschling, D. E.; Simon, J. A. Identification of a small molecule inhibitor of Sir2p. *Proc. Natl. Acad. Sci. U.S.A.* **2001**, *98*, 15113−15118.
(15) Tervo, A. J.; Kyrylenko, S.; Niskanen, P.; Salminen, A.; Leppanen, J. et al. An in silico approach to discovering novel inhibitors of human sirtuin type 2. *J. Med. Chem.* **2004**, *47*, 6292−6298.
(16) Napper, A. D.; Hixon, J.; McDonagh, T.; Keavey, K.; Pons, J. F. et al. Discovery of indoles as potent and selective inhibitors of the deacetylase SIRT1. *J. Med. Chem.* **2005**, *48*, 8045−8054.
(17) Howitz, K. T.; Bitterman, K. J.; Cohen, H. Y.; Lamming, D. W.; Lavu, S. et al. Small molecule activators of sirtuins extend Saccharomyces cerevisiae lifespan. *Nature* **2003**, *425*, 191−196.
(18) Knockaert, M.; Wieking, K.; Schmitt, S.; Leost, M.; Grant, K. M. et al. Intracellular Targets of Paullones. Identification following affinity purification on immobilized inhibitor. *J. Biol. Chem.* **2002**, *277*, 25493−25501.
(19) Goodford, P. J. A computational procedure for determining energetically favorable binding sites on biologically important macromolecules. *J. Med. Chem.* **1985**, *28*, 849−857.
(20) Heltweg, B.; Trapp, J.; Jung, M. In vitro assays for the determination of histone deacetylase activity. *Methods* **2005**, *36*, 332−337.
(21) Wegener, D.; Wirsching, F.; Riester, D.; Schwienhorst, A. A fluorogenic histone deacetylase assay well suited for high-throughput activity screening. *Chem. Biol.* **2003**, *10*, 61−68.
(22) Wegener, D.; Hildmann, C.; Riester, D.; Schwienhorst, A. Improved fluorogenic histone deacetylase assay for high-throughput screening applications. *Anal. Biochem.* **2003**, *321*, 202−208.
(23) Davis, P. D.; Elliott, L. H.; Harris, W.; Hill, C. H.; Hurst, S. A. et al. Inhibitors of protein kinase C. 2. Substituted bisindolylmaleimides with improved potency and selectivity. *J. Med. Chem.* **1992**, *35*, 994−1001.
(24) Ishii, H.; Jirousek, M. R.; Koya, D.; Takagi, C.; Xia, P. et al. Amelioration of vascular dysfunctions in diabetic rats by an oral PKC beta inhibitor. *Science* **1996**, *272*, 728−731.
(25) Goekjian, P. G.; Jirousek, M. R. Protein kinase C in the treatment of disease: signal transduction pathways, inhibitors, and agents in development. *Curr. Med. Chem.* **1999**, *6*, 877−903.
(26) Marmy-Conus, N.; Hannan, K. M.; Pearson, R. B. Ro 31−6045., the inactive analogue of the protein kinase C inhibitor Ro 31−8220., blocks in vivo activation of p70(s6k)/p85(s6k): implications for the analysis of S6K signalling. *FEBS Lett.* **2002**, *519*, 135−140.
(27) Toullec, D.; Pianetti, P.; Coste, H.; Bellevergue, P.; Grand-Perret, T. et al. The bisindolylmaleimide GF 109203X is a potent and selective inhibitor of protein kinase C. *J. Biol. Chem.* **1991**, *266*, 15771−15781.
(28) Davis, P. D.; Hill, C. H.; Lawton, G.; Nixon, J. S.; Wilkinson, S. E. et al. Inhibitors of protein kinase C. 1. 2,3-Bisarylmaleimides. *J. Med. Chem.* **1992**, *35*, 177−184.
(29) Davies, S. P.; Reddy, H.; Caivano, M.; Cohen, P. Specificity and mechanism of action of some commonly used protein kinase inhibitors. *Biochem. J.* **2000**, *351*, 95−105.
(30) Schultz, C.; Link, A.; Leost, M.; Zaharevitz, D. W.; Gussio, R. et al. Paullones, a series of cyclin-dependent kinase inhibitors: synthesis, evaluation of CDK1/cyclin B inhibition, and in vitro antitumor activity. *J. Med. Chem.* **1999**, *42*, 2909−2919.
(31) Kaeberlein, M.; McDonagh, T.; Heltweg, B.; Hixon, J.; Westman, E. A. et al. Substrate specific activation of sirtuins by resveratrol. *J. Biol. Chem.* **2005**, *280*, 17038−17045.
(32) Borra, M. T.; Smith, B. C.; Denu, J. M. Mechanism of human SIRT1 activation by resveratrol. *J. Biol. Chem.* **2005**, *280*, 17187−17195.
(33) Faul, M. M.; Winneroski, L. L.; Krumrich, C. A. Synthesis of Rebeccamycin and 11-Dechlororebeccamycin. *J. Org. Chem.* **1999**, *64*, 2465−2470.
(34) Liu, Z. Design and Synthesis of Conformationally Restricted Indole-Fluorinated Macrocyclic Bis(indolyl)maleimides. M.Sc. Thesis, Mississippi State University, 2001.
(35) Goekjian, P. G.; Wu, G.-Z.; Chen, S.; Zhou, L.; Jirousek, M. R. et al. The Synthesis of Fluorinated Macrocyclic Bis(indolyl)maleimides as Potential 19F-NMR Probes for PKC. *J. Org. Chem.* **1999**, *64*, 4238−4246.
(36) Finnin, M. S.; Donigian, J. R.; Pavletich, N. P. Structure of the histone deacetylase SIRT2. *Nat. Struct. Biol.* **2001**, *8*, 621−625.
(37) Avalos, J. L.; Bever, K. M.; Wolberger, C. Mechanism of sirtuin inhibition by nicotinamide: altering the NAD(+) cosubstrate specificity of a Sir2 enzyme. *Mol. Cell* **2005**, *17*, 855−868.
(38) Zhao, K.; Harshaw, R.; Chai, X.; Marmorstein, R. Structural basis for nicotinamide cleavage and ADP-ribose transfer by NAD(+)-dependent Sir2 histone/protein deacetylases. *Proc. Natl. Acad. Sci. U.S.A.* **2004**, *101*, 8563−8568.
(39) Denu, J. M. The Sir2 family of protein deacetylases. *Curr. Opin. Chem. Biol.* **2005**.
(40) Jones, G.; Willet, P.; Glen, R. C.; Leach, A. R.; Taylor, R. Development and validation of a genetic algorithm for flexible docking. *J. Mol. Biol.* **1997**, *267*, 727−748.
(41) Komander, D.; Kular, G. S.; Schuttelkopf, A. W.; Deak, M.; Prakash, K. R. et al. Interactions of LY333531 and other bisindolyl maleimide inhibitors with PDK1. *Structure* **2004**, *12*, 215−226.
(42) Tame, J. R. Scoring functions−the first 100 years. *J. Comput.-Aided Mol. Des.* **2005**, *19*, 445−451.
(43) North, B. J.; Marshall, B. L.; Borra, M. T.; Denu, J. M.; Verdin, E. The human Sir2 ortholog, SIRT2, is an NAD+-dependent tubulin deacetylase. *Mol. Cell* **2003**, *11*, 437−444.
(44) Guarente, L. Sir2 links chromatin silencing, metabolism, and aging. *Genes Dev.* **2000**, *14*, 1021−1026.
(45) Han, Z.; Pantazis, P.; Lange, T. S.; Wyche, J. H.; Hendrickson, E. A. The staurosporine analog, Ro-31−8220., induces apoptosis independently of its ability to inhibit protein kinase C. *Cell Death Differ.* **2000**, *7*, 521−530.
(46) Kunick, C. Synthese von 7,12-Dihydro-indolo[3,2-d][1]benzazepin-6(5H)-onen und 6,11-Dihydro-thieno-[3′,2′:2,3]azepino[4,5-b]indol-5(4H)-on. *Arch. Pharm.* **1992**, *325*, 297−299.

(47) Joyce, R. P.; Gainor, J. A.; Weinreb, S. M. Synthesis of the aromatic and monosaccharide moieties of staurosporine. *J. Org. Chem.* **1987**, *52*, 1177−1185.
(48) *Molecular Operating Environment (MOE*); Chemical Computing Group Inc.: Montreal, Quebec, Canada, 2005.
(49) Laskowski, R. A.; MacArthur, M. W.; Moss, D. S.; Thornton, J. M. PROCHECK: A program to check the stereochemical quality of protein structures. *J. Appl. Crystallogr.* **1993**, *26*, 283−291.
(50) Still, W. C.; Tempczyk, A.; Hawley, R. C.; Hendrickson, T. Semianalytical treatment of solvation for molecular mechanics and dynamics. *J. Am. Chem. Soc.* **1990**, *112*, 6127−6129.
(51) North, B. J.; Schwer, B.; Ahuja, N.; Marshall, B.; Verdin, E. Preparation of enzymatically active recombinant class III protein deacetylases. *Methods* **2005**, *36*, 338−345.

JM060118B